JACS
JOURNAL OF THE AMERICAN CHEMICAL SOCIETY
Article
pubs.acs.org/JACS

Gd(DOTAla): A Single Amino Acid Gd-complex as a Modular Tool for High Relaxivity MR Contrast Agent Development

Eszter Boros, Miloslav Polasek, Zhaoda Zhang, and Peter Caravan*

The Athinoula A. Martinos Center for Biomedical Imaging, Department of Radiology, Massachusetts General Hospital, Harvard Medical School, 149 Thirteenth Street, Suite 2301, Charlestown, Massachusetts 02129, United States

ABSTRACT: MR imaging at high magnetic fields benefits from an increased signal-to-noise ratio; however T_1-based MR contrast agents show decreasing relaxivity (r_1) at higher fields. High field, high relaxivity contrast agents can be designed by carefully controlling the rotational dynamics of the molecule. To this end, we investigated applications of the alanine analogue of Gd(DOTA), Gd(DOTAla). Fmoc-protected DOTAla suitable for solid phase peptide synthesis was synthesized and integrated into polypeptide structures. Gd(III) coordination results in very rigid attachment of the metal chelate to the peptide backbone through both the amino acid side chain and coordination of the amide carbonyl. Linear and cyclic monomers (Gd**L1**, Gd**C1**), dimers (Gd_2**L2**, Gd_2**C2**), and trimers (Gd_3**L3**, Gd_3**C3**) were prepared and relaxivities were determined at different field strengths ranging from 0.47 to 11.7 T. Amide carbonyl coordination was indirectly confirmed by determination of the hydration number q for the Eu**L1** integrated into a peptide backbone, $q = 0.96 \pm 0.09$. The water residency time of Gd**L1** at 37 °C was optimal for relaxivity, $\tau_M = 17 \pm 2$ ns. Increased molecular size leads to increased per Gd relaxivity (from $r_1 = 7.5$ for Gd**L1** to 12.9 $mM^{-1}\,s^{-1}$ for Gd_3**L3** at 1.4 T, 37 °C). The cyclic, multimeric derivatives exhibited slightly higher relaxivities than the corresponding linearized multimers (Gd_2**C2**: $r_1 = 10.5$ $mM^{-1}\,s^{-1}$ versus Gd_2**C2**-red $r_1 = 9$ $mM^{-1}\,s^{-1}$ at 1.4 T, 37 °C). Overall, all six synthesized Gd complexes had higher relaxivities at low, intermediate, and high fields than the clinically used small molecule contrast agent [Gd(HP-DO3A)(H_2O)].

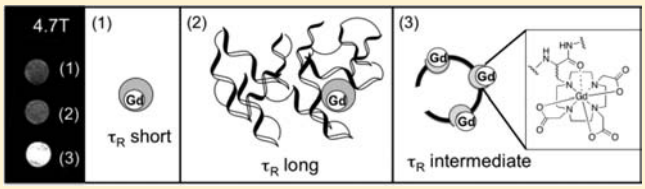

INTRODUCTION

Magnetic resonance imaging (MRI) is one of the most important modalities used for noninvasive investigation of disease in the clinic. MRI is the imaging technology of choice whenever high-resolution tissue contrast is required. Another advantage is the use of harmless magnetic fields for MRI as opposed to ionizing radiation in the case of CT.[1,2]

A large fraction of scans performed in the clinical setting are further enhanced by the use of contrast agents.[3] Contrast agents shorten the relaxation times of water molecules in their proximity and increase tissue contrast on relaxation weighted imaging sequences. Currently, most clinically employed contrast agents are nonspecific, small molecule gadolinium complexes which are able to increase the longitudinal relaxation rate $1/T_1$ of water protons in the extracellular space.[4] The extent to which a contrast agent can enhance relaxation depends on its concentration and its relaxivity (r_1), an inherent property of the molecule. Most approved contrast agents have low relaxivities (r_1) which makes them effective only at relatively high concentrations ($\geq$0.1 mM).[4] There has been a considerable research effort to increase the relaxivity of contrast agents[5−9] Compounds with high relaxivity can be detected at lower doses,[10] or provide greater contrast at equivalent dose to compounds with lower relaxivity. Additionally, an attachment of a targeting moiety allows for target specific delivery of the contrast.[10−12] The clinically approved blood pool agent MS-325 (gadofosveset, Ablavar) is an example of a contrast agent with a high relaxivity;[13,14] this small molecular compound carries an albumin-targeting moiety and will display an over 8 fold increase in relaxivity at low fields once it is associated with human serum albumin (HSA).[15]

While 1.5 T remains the dominant field strength for clinical MRI, there is now a large installed base of 3 T scanners and the major equipment vendors also offer 7 T whole body human scanners. Small animal scanners operate almost exclusively at field strengths of 4.7 T and higher. The primary benefit of high field is the increased signal-to-noise ratio, which enables greater spatial resolution and reduced acquisition time. In addition, the inherent T_1 of tissue increases with increasing magnetic field.[16]

Thus, a contrast agent with equivalent relaxivity at a high and low field would provide much greater contrast at the high field. However, the relaxivity of many T_1-contrast agents decreases more rapidly with applied field than the inherent tissue T_1 increases.

Relaxivity above 0.1 T depends on a variety of parameters, some of which are depicted in Figure 1.[19] As the magnetic field increases, the optimal correlation time, τ_c, for maximum possible relaxivity decreases, as it is inversely dependent on the proton Larmor frequency ω_H. While the contribution from the electronic relaxation time (T_{1e}) is negligible at fields above 1.5 T, contributions from the mean water residency time (τ_M) and the rotational correlation time (τ_R) become the levers for generating high relaxivity Gd-based agents.[20]

For the design of high field, high relaxivity contrast agents it is instructive to consider the equation for two site exchange

Received: September 16, 2012
Published: November 16, 2012

ACS Publications © 2012 American Chemical Society

dx.doi.org/10.1021/ja309187m | J. Am. Chem. Soc. 2012, 134, 19858−19868

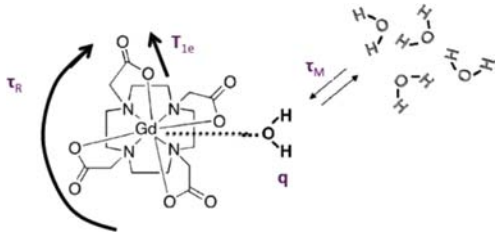

Figure 1. Molecular parameters that influence relaxivity: rotation (τ_R), water exchange (τ_M), hydration number (q) and electronic relaxation (T_{1e}).

written in terms of inner-sphere water relaxivity, eq 1, and the Solomon equation, eq 2, which describes the field dependence of T_1 relaxation of the coordinated inner-sphere water hydrogen atoms.[3] Eq 1 teaches that the inner-sphere water relaxation time T_{1M} and the water residency time, τ_M, should be as short as possible. With regards to T_{1M}, eq 2 indicates that the correlation time should be as large as possible, but while still meeting the requirement of $\omega_H\tau_c < 1$, where ω_H is the proton Larmor frequency and C is a constant. For a given Larmor frequency, there is an optimal correlation time. Unless water exchange is exceedingly fast ($>10^9$ s^{-1}), the correlation time at 1.5 T and higher will essentially be the rotational correlation time, τ_R. If τ_R is very long (nanoseconds and longer), then relaxivity will be very high at low fields, but the condition $\omega_H\tau_c > 1$ will also occur at lower fields and relaxivity will be low at high fields.

$$r_1^{IS} = \frac{q/[H_2O]}{T_{1M} + \tau_M} \quad (1)$$

$$1/T_{1M} = C\left[\frac{3\tau_c}{1 + \omega_H^2\tau_c^2}\right] \quad (2)$$

For instance, MS-325 was designed for high relaxivity at low fields (≤1.5 T). Serum albumin binding of MS-325 results in a very long τ_R resulting in high relaxivity at 1.5 T, but a precipitous decline in relaxivity with increasing field strength.[21,22] Small molecule agents with very short correlation times such as $[Gd(DTPA)(H_2O)]^{2-}$ (Magnevist) display a modest relaxivity decrease with increasing field strength but exhibit relatively low relaxivity due to their rapid tumbling.[23] We have previously investigated the interplay of water exchange and rotational correlation time for Gd-based T_1 agents at fields ranging from 0.47 to 9.4 T,[21] and showed that the optimal ranges are $5 < \tau_M < 25$ ns and $0.5 < \tau_R < 2$ ns to yield high relaxivity over a range of fields. A number of compounds with a corresponding, intermediate τ_R value between 0.35 − 1 ns has been reported,[18,24,25] however none of these structures allow for the simple adjustment of τ_R without sacrificing rigidity of the Gd-complex or complete redesign of the entire scaffold.

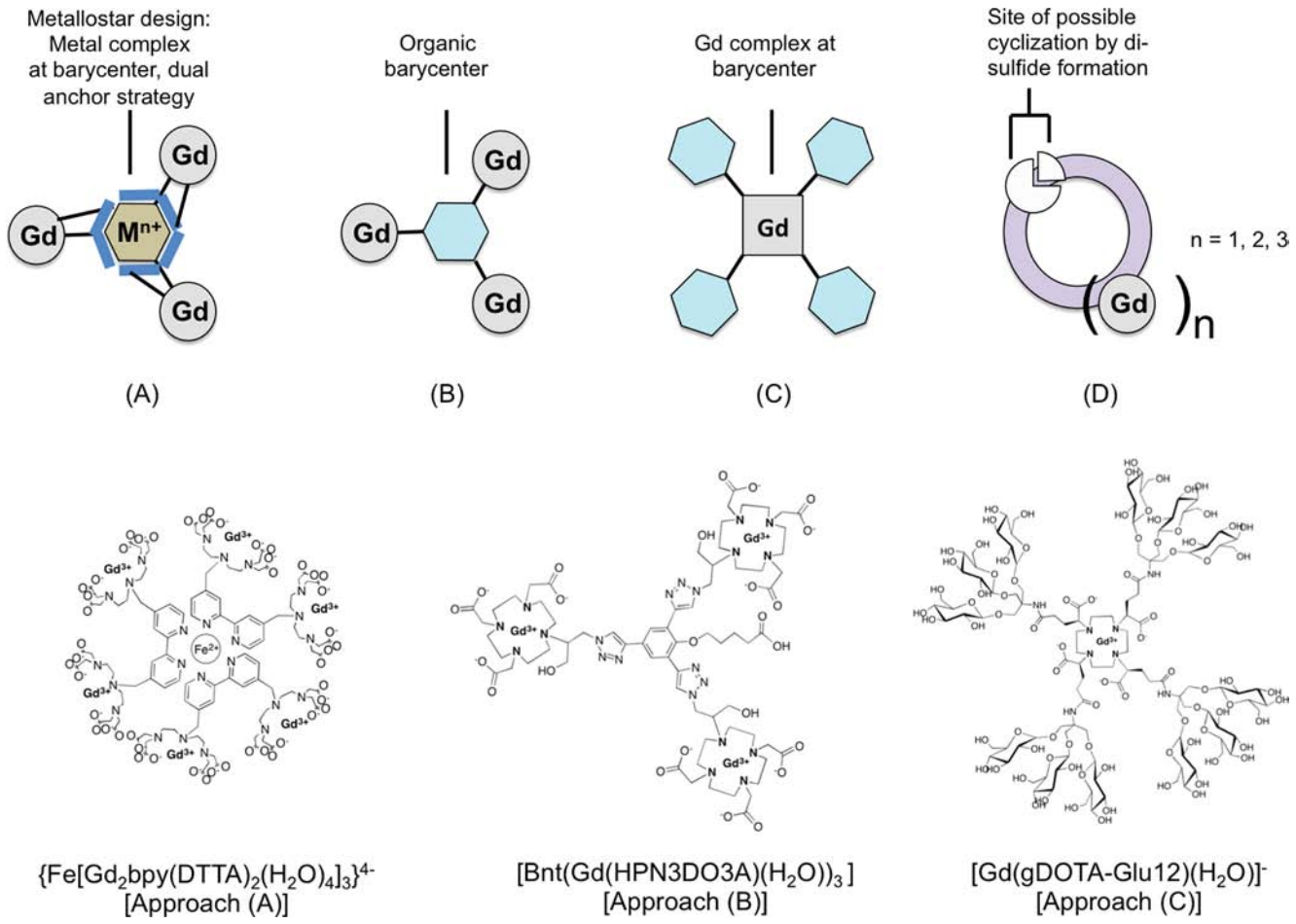

Figure 2. (Top row) Schematic depiction of previously explored Gd complexes with τ_R between 0.35 and 1 ns (A, B, C), as well as the novel approach described here (D). (Bottom row) Examples for molecules reported using approaches A,[17] B[5] and C.[18]

dx.doi.org/10.1021/ja309187m | J. Am. Chem. Soc. 2012, 134, 19858−19868

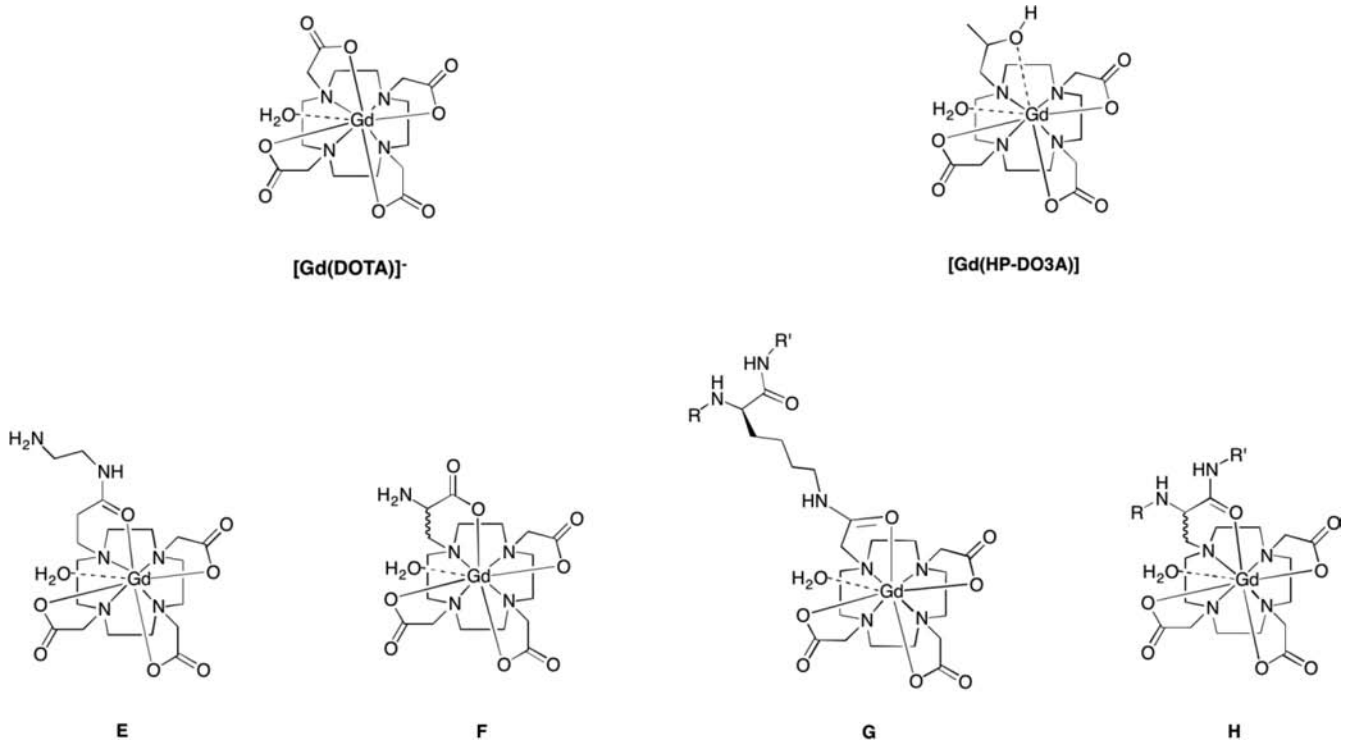

Figure 3. (Top) Structures of approved Gd-based agents $[Gd(DOTA)(H_2O)]^-$ and $[Gd(HP\text{-}DO3A)(H_2O)]$. (Bottom) Various approaches to conjugated DOTA derivates. E and F show previously investigated Gd(DOTA) type complexes with optimal water exchange properties. G represents a previously explored lysine derivative of DOTA without the dual attachment strategy. Compound H represents our approach using dual attachment to the peptide to limit internal motion of the complex.

This paper describes synthesis and investigation of a unique, modular system, capable of the construction of a new generation of high relaxivity T_1 contrast agents for high magnetic fields. Peptide structure and Gd complex incorporation can be easily modified using solid phase peptide synthesis, without change of the local complex environment.

STRUCTURAL DESIGN

Control and optimization of τ_R requires rigid attachment of the corresponding Gd complex to a molecular construct of appropriate size. Conjugating the Gd complex to a targeting vector or molecular scaffold is typically done through a single linkage, and this results in fast internal motion about that linkage and concomitant lower relaxivity. Tweedle and co-workers pioneered the dual anchor strategy,[26] which was also employed by Desreux and colleagues to rigidify attachment of the metal complex for the construction of fatty acid derivatized Gd(DOTA).[27] A similar, multisite attachment strategy was employed for the design of metallostars, where a metallic barycenter is used as a point of attachment for multiple Gd(DTTA) type complexes (Figure 2, approach A).[24] As attachment of multiple copies of the Gd complex increases size, the enhancement of τ_R combined with increase of the Gd-complex payload will further expedite molecular relaxivity.[25,28,29] Meade and colleagues employed click chemistry to attach multiple Gd complexes to rigid, all-organic barycenters (Figure 2, approach B).[5,25] Alternatively, Parker and co-workers showed that the rigid Gd complex can itself be placed at the barycenter of a molecule of variable size (Figure 2, approach C).[18] Most of these constructs display enhanced relaxivity at high fields compared to systems with either very short or very long τ_R. We concluded that a combination of (1) rigid attachment of the metal complex using the dual anchor strategy, (2) multimerization and (3) easy adjustment of molecular size would provide a construct highly suitable for high field applications.

The immediate coordination environment around the Gd ion influences important parameters such as kinetic inertness and water exchange kinetics. While $q \geq 2$ complexes can provide great relaxivity enhancement due to two or more possible sites of interaction for water molecules with the paramagnetic metal,[30−34] only few have the kinetic inertness with respect to Gd dissociation/transchelation required for *in vivo* applications. For $q = 1$, a myriad of kinetically inert Gd(DOTA) type complexes have been well characterized and provided us with the information necessary for choosing a suitable system.[35,36]

DOTA monoproponiamide derivatives, where the amide oxygen atom forms a 6-membered chelate ring upon coordination of Gd(III), were found to have a mean water residency time of 10−20 ns (at 37 °C), which is within the ideal range required for our purposes (Figure 3, compound E).[37] Geraldes and co-workers have reported the synthesis and investigation of Gd(DO3A-*N*-α-aminopropionate) (Figure 3, Compound F).[38] This system provided the basis for our investigations. We reasoned that derivatization and multimerization of DO3A-*N*-α-amino-propionate could be achieved by using an Fmoc-analogue of this system and standard peptide synthesis, similar to an approach previously explored by Sherry and co-workers (Figure 3, compound G),[39] as well as by Stephenson et al.[40] In our system, the complex is linked to the peptide backbone via the short methylene linkage of the alanine side chain. Gadolinium coordination of the amide carbonyl, which is also used for coupling to the polypeptide, provides the second point of attachment and results in a rigid incorporation

Scheme 1. Synthesis of Compound 6

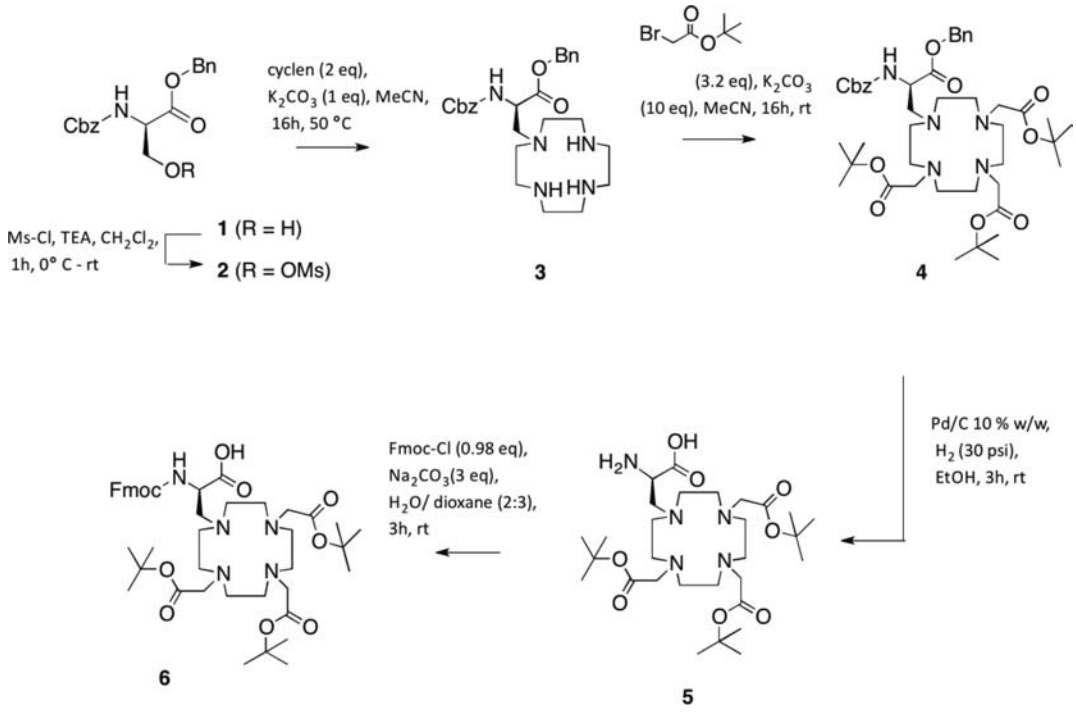

Scheme 2. Synthesis of New Contrast Agents Described in This Paper[a]

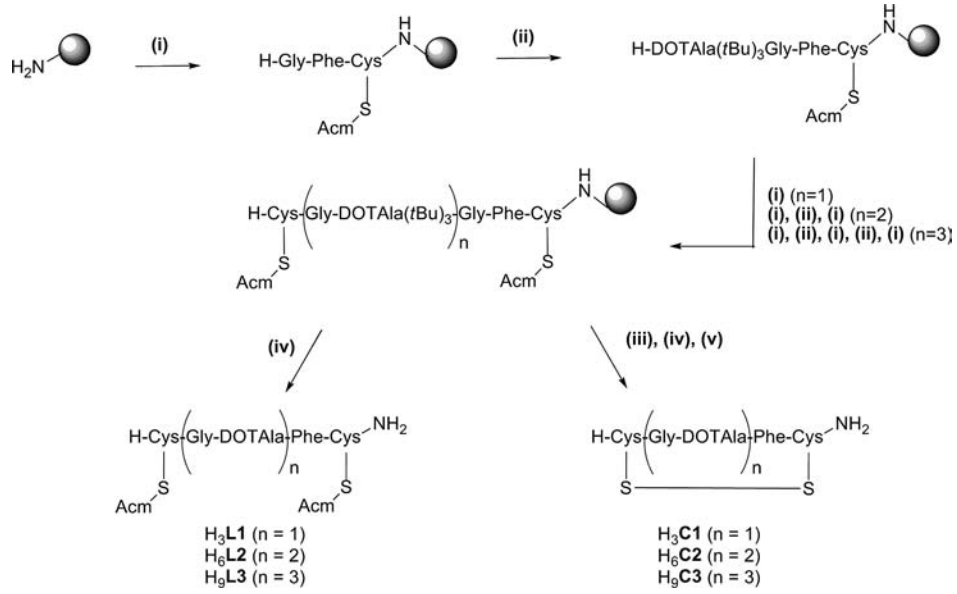

[a](i) (1) 4 equiv Fmoc-X (X = Gly, Phe, Cys(Acm)), 4 equiv HATU, 4.5 equiv NMM, DMF, 12 h, (2) 20% piperidine in DMF, 2 h; (ii) (1) 1.5 equiv **6**, 2 equiv HATU, 3 equiv NMM, (2) 20% piperidine in DMF; (iii) 10 equiv I_2, DMF, 6 h; (iv) TFA/DDT/TIPS/Water (9.5:0.25:0.25:0.25), 6 h; (v) DMSO (2% v/v), H_2O (pH 8), 12 h.

of the complex into the polypeptide that should restrict internal motion and enable control over τ_R. This design would be capable of satisfying all our criteria: fast water exchange, tunable rotational dynamics; limited internal motion, and ease of derivatization using solid phase synthesis. Moreover, by using the Gd(DOTAla) moiety itself to increase molecular size, the overall molecular relaxivity is increased via multimerization (Figure 3, compound H).

RESULTS AND DISCUSSION

Synthesis of Fmoc-DOTAla. For the use of DO3A-*N*-*α*-aminopropionate in solid phase peptide synthesis, construction of the corresponding Fmoc-derivative ("Fmoc-DOTAla-^{t}Bu$_3$", compound **6**) was required. Fmoc is easily deprotected under mildly basic conditions while the ligand-carboxylates remain protected[41] hence it is more suitable for our purposes than a potential Boc-derivative.[5] As cyclen has high inherent basicity, the Fmoc protective group can only be introduced after alkylation of all secondary amines on cyclen.

dx.doi.org/10.1021/ja309187m | J. Am. Chem. Soc. 2012, 134, 19858−19868

We employed a synthetic strategy similar to the one used by Sherry and co-workers[39] in order to afford **6** in 15% over all yield after 5 synthetic steps (Scheme 1). Commercially available serine derivative **1** was converted into the mesylate **2**. Our initial attempted introduction of this sterically crowded synthon onto commercially available *t*-butyl protected DO3A failed. Instead, **2** was used for the mono-*N*-alkylation of cyclen. Compound **3** was further alkylated after removal of excess cyclen mesylate salt using *tert*-butyl bromoacetate in order to afford compound **4**, which was isolated using preparative HPLC. Simultaneous removal of the benzyl and carboxybenzyl protective groups using H_2 and Pd/C yielded compound **5**. Using Fmoc-Cl in a mixuture of H_2O and dioxane under basic conditions for **5** results in the introduction of the desired Fmoc protective group. Compound **6** is purified using preparative HPLC. It was found that using extended reaction times over 12 h leads to a considerable amount of side products of which some are more difficult to separate from the final product.

Synthesis and Evaluation of Monomeric Metallopeptide. As a next step, we aimed to incorporate **6** into the linear model sequence H-Cys(Acm)-Gly-DOTAla-Gly-Phe-Cys(Acm)-NH_2 (H_3**L1**, Scheme 2). The corresponding Gd(III) complex would allow us to study water exchange kinetics, while the analogous Eu(III) complex provides information on the hydration number (q) at the metal center. Rather forcing conditions encompassing HATU in the presence of NMM in DMF were required for significant product formation. We synthesized H_3**L1** using PEGA-Rink resin and standard manual solid phase synthesis (Scheme 2). Incorporation of a Phe residue was employed to provide a UV handle for detection and purification. Two Cys residues were used as the terminal amino acids, serving as potential sites of secondary structure modification through intramolecular disulfide bond formation. The *tert*-butyl esters were removed simultaneously with cleavage from the resin using a typical acidic cleavage cocktail (TFA/DDT/TIPS/H_2O (9.25:0.25:0.25:0.25)). The crude peptide H_3**L1** was isolated using ether precipitation. Complexation with either $GdCl_3{\cdot}6H_2O$ or $EuCl_3{\cdot}6H_2O$ by mixing of aqueous solutions of the metal salt and the crude peptide at pH 3, followed by slow adjustment of the pH to 6.5 using an aqueous 0.1 M NaOH solution yielded the corresponding crude metal complex. The metallopeptide was purified using preparative HPLC.

This class of Ln-DOTA derivatives is typically 9-coordinate. If the amide carbonyl from the peptide backbone was coordinated to the lanthanide, then we would expect a single aqua coligand, that is, q = 1. The luminescence lifetime of the Eu(III) complex was measured in H_2O and D_2O. A custom-designed multimodal confocal imaging system built by Yaseen et al.[42] was used to measure the luminescence lifetime of the Eu(III) excited state $^5D_1$ as previously reported.[43] Luminescence lifetimes were measured and averaged and used for the modified Horrocks equation[44] (eq 3), which accounts for the amide donor as one of the ligands.

$$q_{H_2O} = 1.2\left[\left(\frac{1}{\tau_{H_2O}} - \frac{1}{\tau_{D_2O}}\right) - 0.325\right] \quad (3)$$

The value obtained for the hydration number q was 0.96 ± 0.09, which suggests that the carbonyl of the peptide backbone is indeed coordinated to the metal ion.

Water exchange kinetics for the inner-sphere water ligand were determined by measurement of the temperature dependence of the transverse relaxation time T_2 of $H_2{}^{17}O$ in the presence and absence of Gd**L1**. The data in Figure 4 were fit to a 4 parameter model as described previously.[22] The water exchange rate at 310 K, $^{310}k_{ex}$, its activation enthalpy, $\Delta H^{\ddagger}$, the electronic relaxation time at 310 K, $^{310}T_{1e}$, and its activation energy, $\Delta E^{\ddagger}$ were iteratively varied to fit the observed reduced relaxation rate data R_{2r}. The hyperfine coupling constant was fixed at 3.8×10^6 rad/s.[45] At the high field used, τ_M dominates the scalar correlation time and results in an accurate estimate of water exchange, while the relative contribution of T_{1e} to ^{17}O nuclear relaxation is much lower and this parameter is less well-defined, Table 1. The water residency time ($\tau_M = 1/k_{ex}$) was determined to be 17 ± 2 ns at 310 K, which is similar to the Gd-DOTA-monopropionamide derivative reported by Geraldes and co-workers (Table 1, Figure 4).[38] This similar water exchange rate is also consistent with the amide carbonyl as a donor. We further note that this water residency time is in the optimal range for high relaxivity at all field strengths.

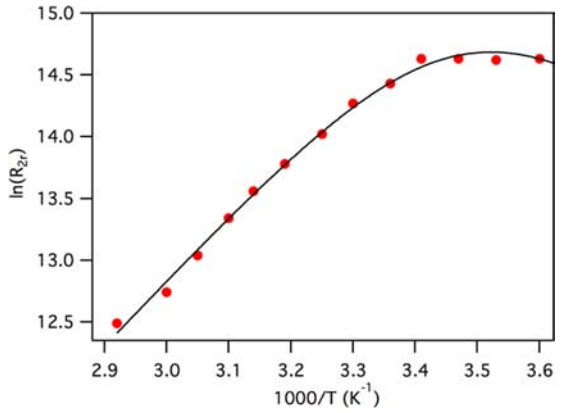

Figure 4. Temperature dependence of the ^{17}O NMR (11.7 T) reduced transverse relaxation rates of GdL1 (6.8 mM). Solid line represents fit to the data to determine the water exchange rate.

Table 1. Water Exchange Kinetic Parameters for GdL1 and Comparison with the Gd(III) Complexes of Propionamide and Propionate Derivatives E and F (Figure 3)[a]

Gd complex	E[37]	F[38]	Gd**L1**
$^{310}k_{ex} \times 10^6$ (s^{-1})	84	42	60 ± 6
$\Delta H^{\ddagger}$ (kJ mol^{-1})	34.0	19.1	41.7 ± 3.2
$^{310}\tau_M$ (ns)	12	24	17 ± 2

[a] $^{310}T_{1e}$ = 160 ± 124 ns and $\Delta E^{\ddagger}$ = 21 ± 18 kJ mol^{-1} for Gd**L1**.

Multimeric Metallopeptides. Gd**L1** demonstrated that the GdDOTAla moiety could be incorporated into a peptide, and the resultant complex had the expected single inner-sphere water coligand with an optimal water exchange rate. However Gd**L1** is still a rather small molecule with a relatively short τ_R. In order to increase τ_R and enhance the molecular relaxivity, we also synthesized dimeric and trimeric structures. The cysteines were either left protected ("linear" structures) or were deprotected and used to induce intramolecular cyclization ("cyclic" structures) in order to highlight the possibility of secondary structure modification with our approach (Scheme 2). Multimers H_6**L2** and H_9**L3** were furnished using the same synthesis methodology as for the linear, model monomer peptide H_3**L1**. On-bead deprotection of the Acm protective group on the Cys amino acids using I_2 was done in order to

afford the cyclized analogues H_6**C1**, H_6**C2** and H_9**C3**.[46] As cyclization was only 60% complete for compounds H_6**C2** and H_9**C3**, cyclization was driven to completion using 2% DMSO in H_2O at pH 8 (Scheme 2).[47] The Gd complexes Gd**L1**, Gd_2**L2** Gd_3**L3**, Gd**C1**, Gd_2**C2** and Gd_3**C3** were formed and purified using the same methodology as described for the monomer. Isolated yields for the cyclic products were considerably lower due to intermolecular disulfide bond formation resulting in polymeric side products, which are separated by HPLC purification. All Gd complexes were characterized using LC–ESI-MS.

Kinetic Inertness. The development of new contrast agents requires compounds with high thermodynamic stability and kinetic inertness with respect to Gd dechelation. Tei et al. showed that a GdDOTA-monoproponiamide deriviative had a very high stability constant, log K_{ML} = 20.2,[37] and we expected that our system with the same donor set would exhibit similar thermodynamic stability. To address kinetic inertness, we measured the full transchelation of Gd(III) from the complexes Gd**L1**, Gd_2**L2** Gd_3**L3** to a DTPA derivative with higher thermodynamic stability. Each of these complexes was challenged with one equivalent of the ligand of MS-325 (MS-325-L) on a per gadolinium basis (e.g., Gd_3**L3** was challenged with 3 equivalents of MS-325-L). MS-325-L is a DTPA derivative with a biphenyl moiety that enables easy separation and monitoring of the free ligand from the MS-325 gadolinium complex by HPLC. Figure 5 shows the conversion of MS-325-L to MS-325 as a function of time for the three metallopeptides at pH 3 (10 mM citrate buffer) and 37 °C.[48]

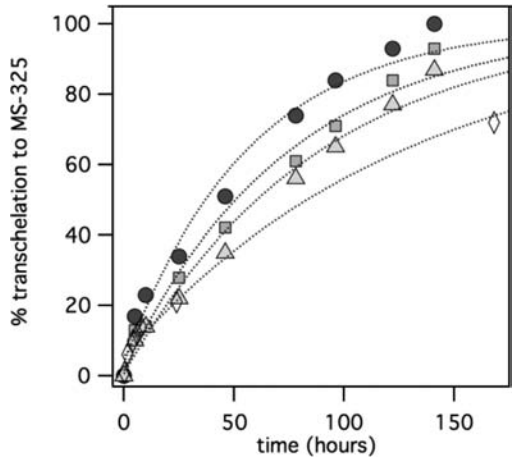

Figure 5. Kinetic inertness of Gd(DOTAla) derivatives. Transchelation of Gd from linear complexes Gd**L1**(●), Gd_2**L2**(■), Gd_3**L3** (▲) and [Gd(HP-DO3A)(H_2O)] (◆) to MS-325 at pH 3, 37 °C. Data shown for the first 168 h of the reaction.

Transchelation was monitored using LC-MS, via formation of the MS-325 complex. For comparison, we also measured transchelation from the approved contrast agents [Gd(HP-DO3A)(H_2O)] (ProHance, gadoteridol) and [Gd(DTPA)-(H_2O)]$^{2-}$ (Magnevist, gadopentetate). Although thermodynamically favored, it is apparent from Figure 5 that transchelation takes place over days even at pH 3. We estimated half-times for these transchelations (time to 50% of the equilibrium value). For the approved contrast agent [Gd-(DTPA)(H_2O)]$^{2-}$, the half-time was 25 min. On the other hand, the metallopeptides were much more inert with half-time in the 2–3 day range (Table 2). Transchelation was slowest for the trimer, followed by the dimer. The approved macrocyclic agent [Gd(HP-DO3A)(H_2O)] showed even slower transchelation kinetics. These results allowed us to conclude that multimers based on Gd(DOTAla) are also suitable for *in vivo* applications due to satisfactory kinetic inertness in comparison with clinically utilized Gd based agents. We were also able to confirm that multimerization has no detrimental effect on decomplexation of the metal complex, rather it appears to have a stabilizing effect.

Table 2. Half-times for Gd Transchelation to MS-325 at pH 3, 37 °C, with a Gd/MS-325-L ratio of 1:1 at 0.1 mM Gd Complex Concentration

Gd complex	$t_{1/2}$ (h)
Gd**L1**	39 ± 3
Gd_2**L2**	52 ± 3
Gd_3**L3**	61 ± 4
Gd(DO3A-HP)	91 ± 6
Gd(DTPA)	0.42 ± 0.0.18

Relaxivity. Per Gd relaxivities were determined by measuring T_1 at 37 °C using 20, 60, 200, 400, and 500 MHz spectrometers. Relaxivities for MS-325 (with and without the presence of HSA) as a reference compound with a long τ_R and [Gd(HP-DO3A)(H_2O)] as a reference for very short τ_R were also measured, and all the relaxivity data is tabulated in Table 3, together with results obtained from literature for the compounds with similar estimated τ_R.

At low fields such as 0.47 and 1.4T, the compounds with the highest rotational correlation times (MS-325/HSA and the trimers) exhibit the highest relaxivity. Additional rigidity through cyclization seems to provide only minor relaxivity increase for the dimeric and trimeric systems (Gd_2**C2** and Gd_3**C3**). At intermediate field (4.7 T), only a moderate decrease in relaxivity is observed for the metallopeptides. In comparison, HSA-associated MS-325 exhibits a peak molecular relaxivity of above 40 mM^{-1} s^{-1},[49] followed by rapid decrease in relaxivity upon increase of the magnetic field. Because we use the rigid GdDOTAla amino acid for multimerization, both the per Gd relaxivity and per molecule relaxivity increase with increased molecular size. Figure 6A illustrates this effect where we plot the field dependent molecular relaxivity of Gd**L3** along with that of the approved contrast agents [Gd(HP-DO3A)-(H_2O)] in PBS and MS-325 in the presence of excess HSA. At 0.47 T the molecular relaxivity of Gd_3**L3** is similar to MS-325 in HSA solution. As the field is increased the molecular relaxivity of Gd_3**L3**, with its intermediate rotational correlation time, becomes higher than that of MS-325/HSA: 50% higher at 1.4 T and 350–450% higher at fields from 4.7 to 11.7 T. The molecular relaxivity of Gd_3**L3** is 5- to 11-fold higher than that of [Gd(HP-DO3A)(H_2O)] at all fields measured. On a per Gd basis, the relaxivity of Gd_3**L3** is 50–220% higher than either HSA-bound MS-325 or [Gd(HP-DO3A)(H_2O)] at high fields (4.7–11.7 T), Figure 6B.

In order to further illustrate this, we imaged a series of phantoms at 4.7 T (Figure 7). Water is used as a reference for background, [Gd(HP-DO3A)(H_2O)] as an example of a compound with a short τ_R, and MS-325 bound to HSA as an example of a complex with a long τ_R. Gd_3**L3** is shown at two different concentrations: either equimolar on a per Gd basis, or on a per molecule basis. It is evident that Gd_3**L3** provides better contrast at this field strength then either FDA approved compound, highlighting superiority in performance of our

Table 3. Measured per Gd Relaxivities as a Function of Proton Larmor Frequency at 37 °C for the Linear and Cyclic Systems Described in This Work along with [Gd(HP-DO3A)(H_2O)] and MS-325 Measured in the Presence and Absence of 4.5% Human Serum Albumin (HSA)[a]

	relaxivity [$mM^{-1}\,s^{-1}$] per Gd				
	20 MHz	60 MHz	200 MHz	400 MHz	500 MHz
Gd**L1**	8.1	7.4	7	5.8	4.9
Gd_2**L2**	10.8	9.9	8.3	6.1	4.9
Gd_3**L3**	13.2	12.2	9	6.1	4.7
Gd**C1**	8.3	7.1	7.3	5.1	4.5
Gd_2**C2**	11.4	10.6	7.5	5.7	4.5
Gd_3**C3**	12.7	12.3	9.2	6.6	5.5
[Gd(HP-DO3A)]	4.3	3.2	3.6	3.0	2.9
MS-325	6.8[e]	5.4[e]	5.7	4.8	4.7
MS-325 w HSA	42[e]	23.8[e]	5.0	4.1	3.7
$\{Fe[Gd_2bpy(DTTA)_2(H_2O)_4]_3\}^{4-}$	20.1[b]	26.8[b]	15.9[b]	8.3[b]	n.a.
$[Bnt(Gd(HPN3DO3A)(H_2O))_3]$	~15[c]	15.4[c]	n.a.	4.8[c]	n.a.
$[Gd(gDOTA\text{-}Glu12)(H_2O)]^-$	23.5[d]	~25[d]	n.a.	n.a.	n.a.

[a]For comparison, literature data with examples of compounds A (q = 2),[17] B,[5] C (data obtained at 25 °C)[18] are included. [b]Reference 17. [c]Reference 5. [d]Reference 18. [e]Data at 20 and 60 MHz from ref 22; n.a., data not available.

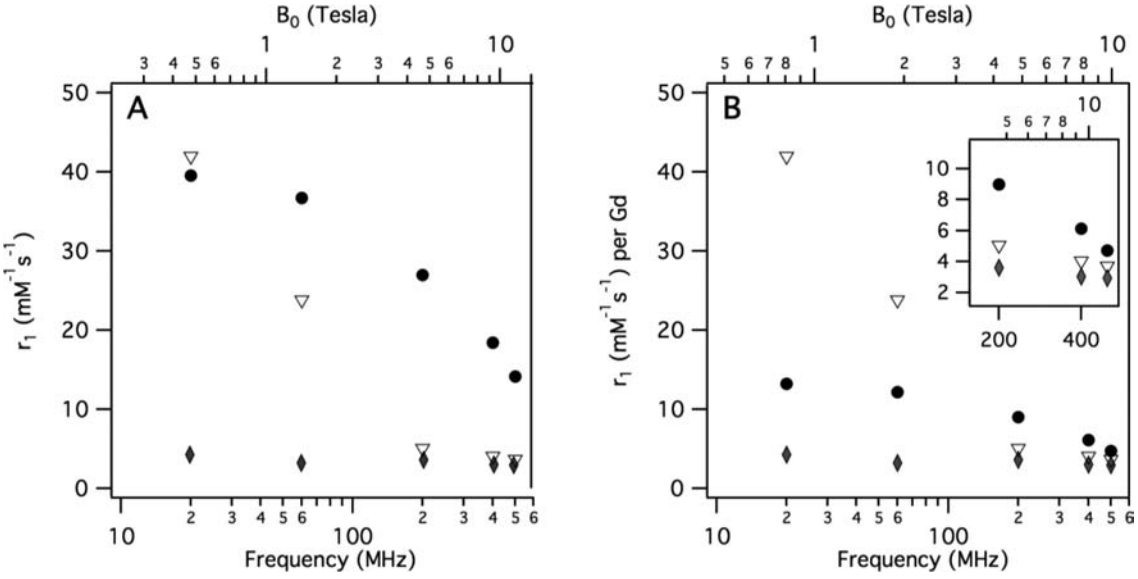

Figure 6. Relaxivities of Gd_3L3(●), MS-325 with excess HSA (∇) and [Gd(HP-DO3A)(H_2O)] (◆) as a function of magnetic field at 37 °C. (A) Relaxivity plotted per molecule showing that Gd_3L3 with its intermediate correlation time is a much more potent relaxation agent than slow or fast tumbling compounds at 60 MHz and higher frequencies. (B) Relaxivity plotted per Gd shows that the intermediate correlation time of Gd_3L3 results in higher relaxivities at high fields.

compound with intermediate τ_R at fields above 1.5 T. Under these conditions, the signal intensity of Gd_3**L3** at equimolar Gd(III) ion concentrations was 65% greater than [Gd(HP-DO3A)(H_2O)] and 55% greater than MS-325/HSA. On a per molecule basis, the Gd_3**L3** phantom was 190% and 170% brighter than Gd(HP-DO3A) and MS-325/HSA, respectively.

At 9.4 T, the per Gd relaxivities were 6.1 and 6.6 $mM^{-1}\,s^{-1}$ for the trimeric metallopeptides. These values are also found to be higher than the relaxivities measured at 9.4 T for previously reported trimeric compounds of similar composition and hydration number.[5,30] For compounds based on q = 2 complexes, higher relaxivities can be obtained.[17]

Investigation of the effect of tertiary structure on relaxivity, was done by examination of the effect of disulfide bond reduction on T_1 at 0.47 and 1.41 T. T_1 was measured for each sample at 37 °C and then the samples were incubated with 20 eq. TCEP for 30 min at room temperature to reduce the intramolecular disulfide bond and give the linear peptide. Subsequently, the T_1 values were remeasured and concentrations redetermined in order to calculate relaxivities. A slight decrease in relaxivity (7−14%) was observed for Gd_2**C2-red** (9 $mM^{-1}\,s^{-1}$) and Gd_3**C3-red** (11.5 $mM^{-1}\,s^{-1}$). Over all, reduction of the disulfide bond has only a slight effect on relaxivity. We hypothesize that the large Gd-chelate side chain and the Gd(III) coordination by the amide carbonyl imposes defined structure to the peptide that dominates the overall molecule structures for both the linear and the cyclic multimers. Introduction of a secondary structure modification such as the cyclization has only a marginal influence on the relaxivity. Nevertheless, facile introduction of the disulfide bridge by use of standard peptide synthesis methodology demonstrates the modularity of our system.

The high field relaxivities that we have obtained are consistent with an intermediate rotational correlation time.

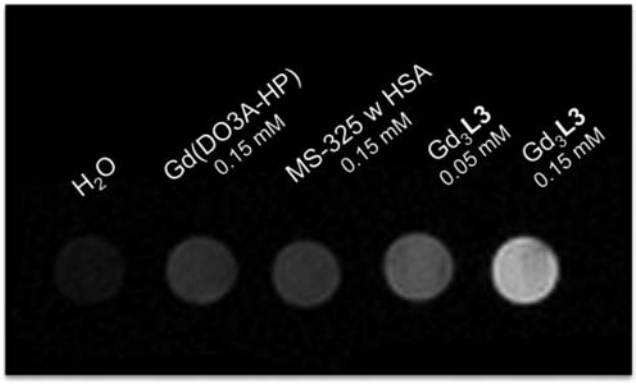

Figure 7. Gradient echo MR image acquired at 4.7 T (T_E = 6 ms and T_R = 30 ms, flip angle = 90°) of equimolar solutions of [Gd(HP-DO3A)(H_2O)], MS-325 in HSA (0.66 mM), Gd_3**L3** in H_2O at both equal Gd(III) ionic concentration and equal molecular concentration.

By assuming that the contributions of second-sphere and outer-sphere water can be estimated from a related q = 0 complex,[50] we estimate τ_R of these metallopeptides to be in 150−600 ps range, based on the magnitude and field dependence of their relaxivities. More precise estimates of τ_R could be obtained by additional relaxation measurements using high resolution NMR with other Ln surrogates of Gd.[51] Compared to the other multimers reported in Table 3, our relaxivities are similar. For a specific field strength the rotational dynamics will dictate the optimal relaxivity. The modular amino acid approach presented here offers the possibility to tune such a high field relaxivity by systematically controlling the size and nuclearity of the complex.

■ CONCLUSIONS

In conclusion, we were able to synthesize a single amino acid Gd chelate, Gd(DOTAla), suitable for solid phase peptide synthesis. The chelate is unique as it provides rigid and stable attachment of the metal complex to the rest of the molecule by using the amido-carbonyl of the corresponding peptide backbone as a point of attachment. Gd(DOTAla) when incorporated into a peptide exhibits one inner-sphere water ligand that has an optimal rate of water exchange for relaxometric purposes. The macrocyclic structure of the chelate provides high thermodynamic stability and kinetic inertness with respect to transchelation or Gd dissociation. The rigid incorporation of Gd(DOTAla) into a peptide scaffold allows design of contrast agents with defined rotational dynamics. Here, we described 6 new compounds containing 1−3 Gd(DOTAla) per peptide in a linear or cyclic peptide framework. By careful control of the rotational dynamics, it is possible to design contrast agents with high relaxivities at both low and high magnetic fields. These new contrast agents were superior to commercial contrast agents [Gd(HP-DO3A)-(H_2O)] and MS-325/HSA at high fields. The modularity of design, the ease of solid phase synthesis, high kinetic inertness, and optimal water exchange rate renders the Gd(DOTAla) scaffold a suitable platform for the development of high field T_1 agents based on Gd.

■ EXPERIMENTAL SECTION

General Methods and Materials. ^{1}H and ^{13}C NMR spectra were recorded on a Varian 11.7 T NMR system equipped with a 5 mm broadband probe. Purification via HPLC of intermediates toward Fmoc-DOTAla was performed using method A: Injection of crude mixture onto preparative HPLC on a Rainin, Dynamax (column: 250 mm Polaris C18) by using A, 0.1% TFA in water; B, 0.1% TFA in MeCN, flow-rate 15 mL/min, from 5% B to 95% B over 20 min. Purification of Gd complexes was performed using method B: Injection of crude mixture onto analytical column (Phenomenex Luna, C18(2) 100/2 mm) using A, water; B, MeCN, flow-rate 0.8 mL/min, 15 min gradient from 2% B to 60% B over 15 min. Monitoring of UV absorption was done at 220 nm. HPLC purity analysis (both UV and MS detection) was carried out on an Agilent 1100 system (column: Phenomenex Luna, C18(2) 100/2 mm) with UV detection at 220, 254, and 280 nm by using a method C: A gradient of 95% A (0.1% formic acid in water) to 95% B (0.1% formic acid in MeCN), flow-rate 0.8 mL/min, over 15 min. Kinetic inertness measurements were also carried out using the LCMS agilent system, using method D: A gradient of 95% A (ammonium formate, 20 mM, pH 6.8) with 5% (9:1 MeCN/20 mm ammonium formate) to 95% B (9:1 MeCN/20 mM ammonium formate), flow-rate 0.8 mL/min, over 15 min.

The synthesis of ligands was carried out as shown in Schemes 1 and 2. Chemicals were supplied by Aldrich Chemical Co., Inc., and were used without further purification. Solvents (HPLC grade) were purchased from various commercial suppliers and used as received.

Luminescence. Measurements were collected by using the confocal portion of a custom-designed multimodal microscope.[42,43] Briefly, a continuous-wave diode laser (l = 532 nm, B&W Tek) provided excitation light that was temporally gated by an electro-optical modulator (ConOptics, Danbury, CT) with extinction ratio of approximately 200 at 532 nm. The excitation beam passed through several conditioning optics, including a beam expander with pinhole spatial filter, polarizer, shutter, dichroic mirror, scan lens, and tube lens and a 20× magnification objective lens (XLumPlan FL, Olympus, NA = 0.95). With the use of a customized control software and galvanometric scanners (Cambridge Technology, Inc. Lexington, MA) the excitation beam was guided to selected locations in the approximately 600 μm field of view. The emitted luminescence was descanned and collected by using an avalanche photodiode photon counting module (APD, SPCM-AQRH-10, Perkin−Elmer, Waltham, MA) sampled at 50 MHz with a high-speed DIO card (National Instruments, Austin, TX). Data were processed by using custom-written software in C and MATLAB (Mathworks, Natick, MA). Detected luminescent photons were binned into 50 ms long bins, to yield time-dependent phosphorescence decay profiles. With the use of a nonlinear least-squares fitting routine, the resulting time-courses were fit with a single-exponential function. A sample's luminescence lifetime is equal to its fitted profile's calculated time constant.

(R)-tritert-Butyl 2,2′,2″-(10-(3-(B)-2-(((benzyloxy)carbonyl)-amino)-3-oxopropyl)-1,4,7,10-tetraazacyclododecane-1,4,7-triyl)-triacetate (4). Cyclen (1.52 g, 8.8 mmol) was dissolved in MeCN (50 mL). K_2CO_3 (1 equiv, 0.61 g) was added and the reaction mixture was preheated to 50 °C. (*R*)-Benzyl 2-(((benzyloxy)carbonyl)amino)-3-((methylsulfonyl)oxy) propanoate (2 equiv, 1.8 g, 4.4 mmol) was dissolved in MeCN (20 mL) and added dropwise to the preheated solution. After 16 h, the precipitate was removed by filtration and the solvent evaporated. The residue was taken up in EtOAc and extracted twice with H_2O (80 mL) and once with brine (80 mL). The organic fraction was dried with Na_2SO_4 and the solvent was evaporated *in vacuo* to afford the crude monocyclen derivative (1.48 g, 3 mmol), which was resuspended in dry MeCN (50 mL) together with K_2CO_3 (10 equiv, 4.24 g). *tert*-Butyl bromoacetate (3.2 equiv, 1.45 mL, 1.91 g) was added dropwise and the mixture was stirred for 16 h at room temperature. The solvent was then removed and the residue was resuspended in EtOAc and extracted with H_2O and brine. The organic fraction was collected, dried with Na_2SO_4 and the solvent was evaporated in vacuo to afford the crude product which was purified using preparative HPLC, method A. Yield: 1.03 g (1.24 mmol, 28%). ^{1}H NMR ($CDCl_3$, 500 MHz, 298 K): δ = 7.31−7.30 (m, Bn−H, 10H), 5.14−5.04 (m, CH_2−Bn, 4H), 4.75 (brs, α-CH, 1H), 3.75−3.05 (m, cyclen-H/N−CH_2−COO^tBu, 24H), 1.47−1.42 (m, CH_3, 27H); ^{13}C NMR ($CDCl_3$, 125 MHz, 303 K): δ = 167.8, 167.7, 160.9, 160.7,

dx.doi.org/10.1021/ja309187m | J. Am. Chem. Soc. 2012, 134, 19858−19868

136.2, 134.8, 128.6, 128.5, 128.2, 127.9, 119.5, 117.2, 114.9, 112.6, 83.3, 68.0, 67.2, 55.0, 54.7, 50.9, 50.15, 27.9; LC/MS (ESI$^+$): $C_{44}H_{67}N_5O_{10}$ m/z: calcd. 826.5 $[M + H]^+$; found: 826.4 $[M + H]^+$.

*(R)-2-Amino-3-(4,7,10-tris(2-(tert-butoxy)-2-oxoethyl)-1,4,7,10-tetraazacyclododecan-1-yl)propanoic Acid (**5**).* Compound **4** (5.5 g, 6.7 mmol) was dissolved in EtOH (600 mL). Pd/C (2.9 g, 10% w/w) was added to afford a slurry which was subjected to H_2 (35 psi) for 3 h. The Pd/C was filtered off and the filtrate was reduced in vacuo to afford the product (3.85 g, 6.4 mmol) as a colorless oil which was used without further purification in the subsequent reaction step. ^{1}H NMR (CD_3OD, 500 MHz, 298 K): δ = 4.18 (brs, α-CH, 1H), 4.85 − 3.15 (m, cyclen-H/N−CH_2−COO^tBu, 24H), 1.53−1.50 (m, CH_3, 27H); ^{13}C NMR (CD_3OD, 125 MHz, 303 K): δ = 170.4, 161.4, 161.2, 83.4, 54.3, 50.1, 49.1, 26.9; LC/MS (ESI$^+$): $C_{29}H_{55}N_5O_8$ m/z: calcd. 602.4 $[M + H]^+$; found: 602.5 $[M + H]^+$.

*(R)-2-((((9H-Fluoren-9-yl)methoxy)carbonyl)amino)-3-(4,7,10-tris(2-(tert-butoxy)-2-oxoethyl)-1,4,7,10-tetraazacyclododecan-1-yl)propanoic Acid (**6**).* Compound **5** (2.395 g, 3.98 mmol) was dissolved in dioxane (60 mL). Na_2CO_3 (1.27 g, 11.9 mmol, 3 equiv) was dissolved in H_2O. The two solutions were mixed and cooled to 0 °C. Fmoc-Cl (1.125 g, 4.3 mmol) was dissolved in dioxane (5 mL) and added to the reaction mixture. The solution was allowed to warm to room temperature and stirred for 4 h. The solvent was then removed and the solid residue was dissolved in MeCN. The residual solid was filtered off and the filtrate was purified using preparative HPLC, method A. The product fractions were pooled and the solvent was removed *in vacuo* to afford the clean product as a white solid (1.81 g, 2.2 mmol, 55%). ^{1}H NMR ($CDCl_3$, 500 MHz, 298 K): δ = 7.30−7.26 (m, FmocAr−H, 10H), 4.76 (brs, α-CH, 1H), 4.30 (m, CH_2−Fmoc, 2H), 4.15 (q, CH-Fmoc, 1H), 3.75−3.05 (m, cyclen-H/N−CH_2−COO^tBu, 24H), 1.45−1.36 (m, CH_3, 27H); ^{13}C NMR ($CDCl_3$, 125 MHz, 303 K): δ = 171.1, 169.7, 143.6, 141.2, 127.8, 127.2, 125.2, 119.9, 84.8, 83.3, 67.5, 54.0, 50.7, 48.3, 46.8, 27.8; LC/MS (ESI$^+$): $C_{44}H_{65}N_5O_{10}$ m/z: calcd. 824.5 $[M + H]^+$; found: 824.4 $[M + H]^+$.

Solid-phase Peptide Synthesis. Solid-phase peptide synthesis was carried out manually following standard Fmoc protocols using PEGA Rink amide resin. All peptide sequences were derived from one solid support 0.33 mmol scale using single step couplings of four equivalents of Fmoc-amino acids, two equiv of coupling agent (HATU) and 3 equiv of *N*-methylmorpholine (NMM) in DMF at RT (refer to Scheme 2). Coupling with commercial amino acids was completed within 12 h (Step i), while Fmoc-DOTAla was only used in a 1.5 equiv excess and allowed to react with the free N terminus of the peptide for 48 h (Step ii). The coupling step was followed by rinsing with DMF and deprotection with 20% piperidine in DMF for 2 h. After subsequent thorough rinsing with DMF and dichloromethane, a small aliquot of solid support was removed from the batch and deprotected using cleavage cocktail (TFA/DDT/TIPS/Water (9.25:0.25:0.25:0.25)) room temperature for 2 h. The resin was filtered off and the filtrate concentrated with a gentle nitrogen flow. The intermediate was precipitated with cold diethyl ether, collected and characterized by ESI-MS. If coupling was found to be complete, the next coupling step was initiated on the main peptide batch. Once a sequence was complete, the corresponding aliquot was removed from the main resin batch and completed by addition of the terminal Fmoc-Cysteine-S-Acm. For cyclic sequences, treating the resin-bound peptide with 10 equiv of I_2 in DMF for 6 h completed side chain deprotection with simultaneous cyclization of the Cys residues (Step iii). After thorough rinsing of the resin with DMF and dichloromethane following the final processing step on-bead (Fmoc deprotection for linear systems, I_2 cyclization for cyclic sequences), the crude peptide was afforded by cleaving from the resin using the acidic cleavage cocktail (see above) and isolated by cold ether precipitation, redissolution in water and lyophilization (Step iv). Because the on-bead cyclization proceeds to only approximately 60% completion, the crude peptide is further cyclized using 2% DMSO in basic H_2O (pH ∼7.5). As epimerization occurs on the stereocenter of DOTAla, multiple peaks are detected for the corresponding diastereomers.

H_2N−C(Acm)PG-DOTAla-GC(Acm)$CONH_2$ (H_3**L1**), HPLC: R_t = 2.4/3.1 min, MS-ESI: m/z: 1043.4 (calcd. 1043.3) $[M + H]^+$.

H_2N−C(Acm)PG-DOTAla-G-DOTAla-GC(Acm)$CONH_2$ (H_6**L2**), HPLC: R_t = 1.3/1.48 min, MS-ESI: m/z: 1514.6 (calcd. 1514.5) $[M + H]^+$.

H_2N−C(Acm)PG-DOTAla-G-DOTAla-G-DOTAla-GC(Acm)-$CONH_2$ (H_9**L3**), HPLC: R_t = 1.21/1.35 min, MS-ESI: m/z: 994.0 (calcd. 994.2) $[M + 2H]^{2+}$.

H_2N−C(S^{cycl})PG-DOTAla-GC(S^{cycl})$CONH_2$ (H_3**C1**), HPLC: R_t = 1.35/1.6 min, MS-ESI: m/z: 898.4 (calcd. 898.3) $[M + H]^+$.

H_2N−C(S^{cycl})PG-DOTAla-G-DOTAla-GC(S^{cycl})$CONH_2$ (H_6**C2**), HPLC: R_t = 1.1/1.2 min, MS-ESI: m/z: 1372.5 (calcd. 1372.3) $[M + H]^+$.

H_2N−C(S^{cycl})PG-DOTAla-G-DOTAla-G-DOTAla-GC(S^{cycl})-$CONH_2$ (H_9**C3**), HPLC: R_t = 1.24 min, MS-ESI: m/z: 922.95 (calcd. 922.8) $[M + 2H]^{2+}$.

Gadolinium Complex Formation. Complexes were prepared by adding $GdCl_3$•$6H_2O$ stock solution to a solution of ligand at pH 3 while stirring. The pH was gradually adjusted to pH 6.5 using 0.1 M NaOH solution. Complete complex formation was checked by LCMS (no residual ligand detectable). The solution was filtered and purified using preparative HPLC, method B. The Eu(III) complex is formed in analogous fashion.

H_2N−C(Acm)PG-DOTAla(Gd)-GC(Acm)$CONH_2$ (Gd**L1**), HPLC: R_t = 2.9/3.3 min, MS-ESI: m/z: 1197.3 (calcd. 1197.2) $[M + H]^+$.

H_2N−C(Acm)PG-DOTAla(Gd)-G-DOTAla(Gd)-GC(Acm)-$CONH_2$ (Gd_2**L2**), HPLC: R_t = 2.6/3.0 min, MS-ESI: m/z 912.5 (calcd. 912.5) $[M + 2H]^{2+}$.

H_2N−C(Acm)PG-DOTAla(Gd)-G-DOTAla(Gd)-G-DOTAla-(Gd)-GC(Acm)$CONH_2$ (Gd_3**L3**), HPLC: R_t = 3.2 min, MS-ESI: m/z: 1225.95 (calcd. 1225.8) $[M + 2H]^{2+}$.

H_2N−C(S^{cycl})PG-DOTAla(Gd)-GC(S^{cycl})$CONH_2$ (Gd**C1**), HPLC: R_t = 1.13 min, MS-ESI: m/z: 1053.2 (calcd. 1053.4) $[M + H]^+$.

H_2N−C(S^{cycl})PG-DOTAla(Gd)-G-DOTAla(Gd)-GC(S^{cycl})-$CONH_2$ (Gd_2**C2**), HPLC: R_t = 1.25 min, MS-ESI: m/z 840.7 (calcd. 841.5) $[M + 2H]^{2+}$.

H_2N−C(S^{cycl})PG-DOTAla(Gd)-G-DOTAla(Gd)-G-DOTAla-(Gd)-GC(S^{cycl})$CONH_2$ (Gd_3**C3**), HPLC: R_t = 1.35/1.9 min, MS-ESI: m/z: 1153.8 (calcd. 1154.6) $[M + 2H]^{2+}$.

Reduction of Disulfide Bond for Relaxivity Measurements. Complex solutions of purified, cyclic Gd complexes (concentrations of 0.1−0.025 mM, 110 μL) in HEPES buffer (50 mM, pH 7.4) were mixed with TCEP solution (20 mM in HEPES, 10 μL) and incubated room temperature. Reduction was checked by LCMS analysis and found to be complete after 30 min.

H_2N−C(SH)PG-DOTAla(Gd)-GC(SH)$CONH_2$ (Gd**C1-red**), HPLC: R_t = 2.35 min, MS-ESI: m/z: 1055.2 (calcd. 1055.2) $[M + H]^+$.

H_2N−C(SH)PG-DOTAla(Gd)-G-DOTAla(Gd)-GC(SH)-$CONH_2$ (Gd_2**C2-red**), HPLC: R_t = 2.8−3.1 min, MS-ESI: m/z 841.7 (calcd. 842.0) $[M + 2H]^{2+}$.

H_2N−C(SH)PG-DOTAla(Gd)-G-DOTAla(Gd)-G-DOTAla-(Gd)-GC(SH)$CONH_2$ (Gd_3**C3-red**), HPLC: R_t = 3.1−3.3 min, MS-ESI: m/z: 1155 (calcd. 1155) $[M + 2H]^{2+}$.

Measurement of Kinetic Inertness. Stock solutions of MS-325-L and Gd**L1**, Gd_2**L2** and Gd_3**L3** were prepared in 50 mM citrate buffer at pH 3.0. MS-325-L was added to solutions of the Gd complexes and incubated at 37 °C. The final concentrations of the metal complexes were 0.1 mM, while the concentration of MS-325-L was adjusted according to the amounts of Gd complexes per metallopeptide present. A 10 μL aliquot was removed for HPLC analysis and analyzed while the remainder of the solution was incubated at 37 °C. A 10 μL aliquot was removed and analyzed at 5, 10, 25, 46, 78, 96, 122, 141 and 244 h. As a reference, Gd(HP-DO3A) was subjected to MS-325-L under same conditions and measured at time points 0.3, 1.5, 4, 6, 8, 24, 168 and 336 h.

Measurement of Relaxivity. Longitudinal relaxation times T_1, were measured on Bruker Minispecs mq20 (0.47 T) and mq60 (1.41 T), a Bruker Bioscan horizontal bore 4.7, 9.4 and 11.7 T Varian NMR spectrometers. T_1 was measured by using an inversion recovery

method with 10 inversion time values ranging from 0.05 × T_1 to 5 × T_1. Relaxivity was calculated from a linear plot of 3 or 4 different concentrations (ranging from 0.01 to 0.5 mM, depending on amount of compound isolated) versus the corresponding inverse relaxation times. All samples were measured at 37 °C using either the internal temperature control of the instrument (0.47, 1.41, 9.4, and 11.7 T) or a warm air blower (4.7 T). MS-325/HSA was prepared in a 4.5% w/v solution of HSA (0.66 mM) in PBS. The MS-325 concentration (in presence of HSA) ranged from 0.05 to 0.15 mM.

^{17}O NMR of GdL1 Solution for Determination of τ_M. ^{17}O NMR measurements of solutions were performed at 11.7 T on 150 μL samples contained in 2-mm-shigemi tubes inside a 5 mm standard NMR tube on a Varian spectrometer. Temperature was regulated by air flow controlled by a Varian VT unit. ^{17}O transverse relaxation times of distilled water (pH 3) containing 5% enriched $^{17}OH_2$ or a 6.88 mM solution of Gd**L1** (pH 7.4, 50 mM HEPES buffer) were measured using a CPMG sequence. The concentration of the sample was determined by ICP-MS. Reduced relaxation rates, $1/T_{2r}$ were calculated from the difference of $1/T_2$ between the Gd**L1** sample and the water blank, and then divided by the mole fraction of coordinated water. The temperature dependence of $1/T_{2r}$ was fit to a 4-parameter model as previously described.[22] The Gd–O hyperfine coupling constant, $A/\hbar$, was assumed to be 3.8 × 10^6 rad/s,[45] the Gd–O distance was assumed to be 3.1 Å.[52]

AUTHOR INFORMATION

Corresponding Author

caravan@nmr.mgh.harvard.edu

Notes

The authors declare no competing financial interest.

ACKNOWLEDGMENTS

Dr. Mohammad A. Yaseen is warmly acknowledged for measurement of the luminescence lifetimes of Eu(**L1**). Dr. Daniel Schühle is acknowledged for helpful discussions. This work was supported in part by awards R01EB009062 from the National Institute of Biomedical Imaging and Bioengineering and P41RR14075 from the National Center for Research Resources. E.B. acknowledges the Swiss National Science Foundation for a fellowship for prospective researchers.

REFERENCES

(1) Young, I. R. *Methods in Biomedical Magnetic Resonance Imaging and Spectroscopy*; John Wiley & Sons Ltd.: Chichester, 2000.
(2) Caravan, P. *Acc. Chem. Res.* **2009**, *42*, 851–862.
(3) Caravan, P.; Ellison, J. J.; McMurry, T. J.; Lauffer, R. B. *Chem. Rev.* **1999**, *99*, 2293–2352.
(4) Caravan, P. *Chem. Soc. Rev.* **2006**, *35*, 512–523.
(5) Mastarone, D. J.; Harrison, V. S. R.; Eckermann, A. L.; Parigi, G.; Meade, T. J. *J. Am. Chem. Soc.* **2011**, *133*, 5329–5337.
(6) Garimella, P. D.; Datta, A.; Romanini, D. W.; Raymond, K. N.; Francis, M. B. *J. Am. Chem. Soc.* **2011**, *133*, 14704–14709.
(7) Kielar, F.; Tei, L.; Terreno, E.; Botta, M. *J. Am. Chem. Soc.* **2010**, *132*, 7836–7837.
(8) Costa, J.; Tóth, É.; Helm, L.; Merbach, A. E. *Inorg. Chem.* **2005**, *44*, 4747–4755.
(9) Aime, S.; Frullano, L.; Crich, S. G. *Angew. Chem., Int. Ed.* **2002**, *41*, 1017–1019.
(10) Terreno, E.; Castelli, D. D.; Viale, A.; Aime, S. *Chem. Rev.* **2010**, *110*, 3019–2042.
(11) Raymond, K. N.; Pierre, V. C. *Bioconjugate Chem.* **2005**, *16*, 3–8.
(12) Major, J. L.; Meade, T. J. *Acc. Chem. Res.* **2009**, *42*, 893–903.
(13) Lauffer, R. B.; Parmelee, D. J.; Dunham, S. U.; Ouellet, H. S.; Dolan, R. P.; Witte, S.; McMurry, T. J.; Walovitch, R. C. *Radiology* **1998**, *207*, 529–538.
(14) McMurry, T. J.; Parmelee, D. J.; Sajiki, H. S., D. M.; Ouellet, H. S.; Walovitch, R. C.; Tyeklar, Z.; Dumas, S.; Bernard, P.; Nadler, S.; Midelfort, K.; Greenfield, M.; Troughton, J.; Lauffer, R. B. *J. Med. Chem.* **2002**, *45*, 3465–3474.
(15) Caravan, P.; Cloutier, N. J.; Greenfield, M. T.; McDermid, S. A.; Dunham, S. U.; Bulte, J. W. M.; Amedio, J. C.; Looby, R. J.; Supkowski, R. M.; Horrocks, W. D.; McMurry, T. J.; Lauffer, R. B. *J. Am. Chem. Soc.* **2002**, *124*, 3152–3162.
(16) Rooney, W. D.; Johnson, G.; Li, X.; Cohen, E. R.; Kim, S.-G.; Ugurbil, K.; Springer, C. S. *Magn. Reson. Med.* **2007**, *57*, 308–318.
(17) Livramento, J. B.; Sour, A.; Borel, A.; Merbach, A. E.; Tóth, É. *Chem.—Eur. J.* **2006**, *12*, 989–1003.
(18) Fulton, D. A.; Elemento, E. M.; Aime, S.; Chaabane, L.; Botta, M.; Parker, D. *Chem. Commun.* **2006**, 1064–1066.
(19) Caravan, P.; Zhang, Z. *Eur. J. Inorg. Chem.* **2012**, 1916–1923.
(20) Helm, L. *Future Med. Chem.* **2010**, *2*, 385–396.
(21) Caravan, P.; Farrar, C. T.; Frullano, L.; Uppal, R. *Contrast Media Mol. Imaging* **2009**, *4*, 89–100.
(22) Caravan, P.; Parigi, G.; Chasse, J. M.; Cloutier, N. J.; Ellison, J. J.; Lauffer, R. B.; Luchinat, C.; McDermid, S. A.; Spiller, M.; McMurry, T. J. *Inorg. Chem.* **2007**, *46*, 6632–6639.
(23) Rohrer, M.; Bauer, H.; Mintorovitch, J.; Requardt, M.; Weinmann, H. *Invest. Radiol.* **2005**, *40*, 715–724.
(24) Paris, J.; Gameiro, C.; Humblet, V.; Mohapatra, P. K.; Jacques, V.; Desreux, J. F. *Inorg. Chem.* **2006**, *45*, 5092–5102.
(25) Song, Y.; Kohlmeir, E. K.; Meade, T. J. *J. Am. Chem. Soc.* **2008**, *130*, 6662–6663.
(26) Ranganathan, R. S.; Fernandez, M. E.; Kang, S. I.; Nunn, A. D.; Ratsep, P. C.; Pillai, K. M. R.; Zhang, X.; Tweedle, M. F. *Invest. Radiol.* **1998**, *33*, 779–797.
(27) Vanasschen, C.; Bouslimani, N.; Thonon, D.; Desreux, J. F. *Inorg. Chem.* **2011**, *50*, 8946–8958.
(28) Sieving, P. F.; Watson, A. D.; Rocklage, S. M. *Bioconjugate Chem.* **1990**, *1*, 65–71.
(29) Aime, S.; Botta, M.; Crich, S. G.; Giovenzana, G.; Palmisano, G.; Sisti, M. *Bioconjugate Chem.* **1999**, *10*, 192–199.
(30) Livramento, J. B.; Helm, L.; Sour, A.; O'Neil, C.; Merbach, A. E.; Tóth, É. *Dalton Trans.* **2008**, 1195–1202.
(31) Datta, A.; Raymond, K. N. *Acc. Chem. Res.* **2009**, *42*, 938–947.
(32) Aime, S.; Calabi, L.; Cavallotti, C.; Gianolio, E.; Giovenzana, G. B.; Losi, P.; Maiocchi, A.; Palmisano, G.; Sisti, M. *Inorg. Chem.* **2004**, *43*, 7588–7590.
(33) Mato-Iglesias, M.; Roca-Sabio, A.; Pálinkás, Z.; Esteban-Gómez, D.; Platas-Iglesias, C.; Tóth, É.; Blas, A. d.; Rodríguez-Blas, T. *Inorg. Chem.* **2008**, *47*, 7840–7851.
(34) Tallec, G.; Imbert, D.; Fries, P. H.; Mazzanti, M. *Dalton Trans.* **2010**, *39*, 9490–9492.
(35) Jaszberenyi, Z.; Toth, E.; Kalai, T.; Kiraly, R.; Burai, L.; Brucher, E.; Merbach, A. E.; Hideg, K. *Dalton Trans.* **2005**, 694–701.
(36) Villaraza, A. J. L.; Bumb, A.; Brechbiel, M. W. *Chem. Rev.* **2010**, *110*, 2921–2959.
(37) Tei, L.; Gugliotta, G.; Baranyai, Z.; Botta, M. *Dalton Trans.* **2009**, 9712–9714.
(38) Ferreira, M. F.; Martins, A. F.; Martins, J. A.; Ferreira, P. M.; Toth, E.; Geraldes, C. F. G. C. *Chem. Commun.* **2009**, *43*, 6475–6477.
(39) De Leon-Rodriguez, L. M.; Kovacs, Z.; Dieckmann, G. R.; Sherry, A. D. *Chem.—Eur. J.* **2004**, *10*, 1149–1155.
(40) Stephenson, K. A.; Zubieta, J.; Banerjee, S. R.; Levadala, M. K.; Taggart, L.; Ryan, L.; McFarlane, N.; Boreham, D. R.; Maresca, K. P.; Babich, J. W.; Valliant, J. F. *Bioconjugate Chem.* **2004**, *15*, 128–136.
(41) Vuljanic, T.; Bergquist, K.-E.; Clausen, H.; Roy, S.; Kihlberg, J. *Tetrahedron* **1996**, *52*, 7983–8000.
(42) Yaseen, M. A.; Srinivasan, V. J.; Sakadzic, S.; W. Wu, S. R.; Vinogradov, S. A.; Boas, D. A. *Opt. Express.* **2009**, *17*, 22341–22349.
(43) Moriggi, L.; Yaseen, M. A.; Helm, L.; Caravan, P. *Chem.—Eur. J.* **2012**, *18*, 3675–3686.
(44) Beeby, A.; Clarkson, I. M.; Dickins, R. S.; Faulkner, S.; Parker, D.; Royle, L.; Sousa, A. S. d.; Williams, J. A. G.; Woods, M. *J. Chem. Soc., Perkin Trans.* **1999**, *2*, 493–503.

(45) Powell, D. H.; Dhubhghaill, O. M. N.; Pubanz, D.; Helm, L.; Lebedev, Y. S.; Schlaepfer, W.; Merbach, A. E. *J. Am. Chem. Soc.* **1996**, *118*, 9333−9346.
(46) Xiaobing, T.; Wickstrom, E. *Org. Lett.* **2002**, *4*, 4013−4016.
(47) Annis, I.; Hargittai, B.; Barany, G. *Meth. Enzymol.* **1997**, *289*, 198−221.
(48) Overoye-Chan, K.; Koerner, S.; Looby, R. J.; Kolodziej, A. F.; Zech, S. G.; Deng, Q.; Chasse, J. M.; McMurry, T. J.; Caravan, P. *J. Am. Chem. Soc.* **2008**, *130*, 6025−6039.
(49) Eldredge, H. B.; Spiller, M.; Chasse, J. M.; Greenwood, M. T.; Caravan, P. *Invest. Radiol.* **2006**, 41.
(50) Dumas, S.; Jacques, V.; Sun, W.-C.; Troughton, J. S.; Welch, J. T.; Chasse, J. M.; Schmitt-Willich, H.; Caravan, P. *Invest. Radiol.* **2010**, *45*, 600−612.
(51) Zech, S. G.; Eldredge, H. B.; Lowe, M. P.; Caravan, P. *Inorg. Chem.* **2007**, *46*, 3576−3584.
(52) Caravan, P.; Astashkin, A. V.; Raitsimring, A. M. *Inorg. Chem.* **2003**, *42*, 3972−3974.